August 2020

The Role of Substrate Elasticity in Droplet Splashing

Bailey Basso
Clemson University, bbasso7796@gmail.com

The role of substrate elasticity in droplet splashing

A Dissertation
Presented to
the Graduate School of
Clemson University

In Partial Fulfillment
of the Requirements for the Degree
Master of Science
Mechanical Engineering

---

by
Bailey C. Basso
August 2020

Accepted by:
Dr. Joshua Bostwick, Committee Chair
Dr. John R. Saylor
Dr. Xin Zhao

Abstract

Drop impact onto elastic substrates is important in applications such as spray coating, bio-printing, forensic analysis, and aerosol drug delivery. The dynamics of impact are complex and include a sequence of events that cause a drop to splash or deposit, form a corrugated leading edge with a well-defined number of spines that may or may not pinchoff into satellite drops during spreading, and finally retraction of the main drop to an equilibrium configuration. Careful experiments are performed to quantify droplet impact on soft gel substrates made of either PDMS silicone or gelatin hydrogels of varying elastic modulus. High-speed photography and image processing quantify the splash dynamics. The splash threshold, as defined by the Weber number, increases as the substrate elasticity decreases making it harder to splash on soft substrates. For relatively stiff substrates, the spreading factor agrees with previously literature but there is systematic deviation for the softest substrates indicating that elasticity plays a crucial role in the spreading dynamics. Surprisingly, the retraction dynamics on soft substrates do not show any correlation with the impact velocity for water, but show a complex behavior when using ethanol as the working liquid which can be attributed to the different wetting properties. The reported results agree well with existing literature for most cases and provides new insights for gels with small elasticity.

Dedication

I would like to dedicate this work to my grandparents, who took care of me during the summers when I was young. My initial passion for learning the science behind how things work came from working on their farm and helping my Grandpa tinker in his shed. Also to my parents who never hesitated to give me all I needed to accomplish my dreams and goals.

Acknowledgments

Thank you to Dr. Joshua Bostwick, who provided countless hours of guidance and insight into my project. Thank you to Dr. John Saylor and Dr. Xin Zhao, for their involvement in my committee and their helpful comments while reviewing this work. Thank you to Chase Gabbard, Caleb Wilson, Xingchen Shao, Saiful Tamim, Phillip Wilson, Carlos Perez, Nathan Brown, Steven Iannucci, and Michelle Rodgers for valuable comments and suggestions that have improved this work. Lastly, I would like to thank my mom and dad for the lasting support and encouragement throughout this work.

Table of Contents

List of Tables

List of Figures

Chapter 1

Introduction

1.1 Motivation

Droplet splashing has been studied since the late 19th century when Worthington used novel imaging techniques to illuminate the splash at the moment of impact [57]. Recent advances in high-speed imaging made it possible to reveal a number of different splash morphologies. For example, Edgerton, showed that drops impacting a thin liquid layer produced shapes he referred to as 'coronets' which would later become known as the 'crown splash', as shown in Figure 1.1. A large volume of literature has been devoted to the study of splashing on liquid baths and hard substrates, and impact dynamics are known to be affected by liquid properties, such as surface tension [35], density [45], and viscosity [33] and substrates properties, such as wettability [18], texture or micropatterning [60], stiffness [1, 19, 36], and ambient air pressure [59]. Somewhat surprising given the vast literature is that the study of splashing on soft substrates is relatively unexplored.

Droplet impact onto soft elastic substrates is seen in many different applications. For example, bioprinting technologies exhibit similar dynamics to inkjet printing techniques [52, 22] but adapted for living cells. Tissue scaffolds are built by depositing drops onto soft substrates to manufacture organs. Similarly, aerosol drug delivery in the lungs involves drop impact onto soft tissues and the efficiency of drug delivery is related to the impact dynamics. This is also important to quantify the spread of infectious disease that attaches to the lungs via aerosols [13]. In both such applications, the tissue can be viewed as a soft elastic substrate. Blood splatter analysis has also been used to recreate crime scenes by interpreting the spread and morphology of the drop impact

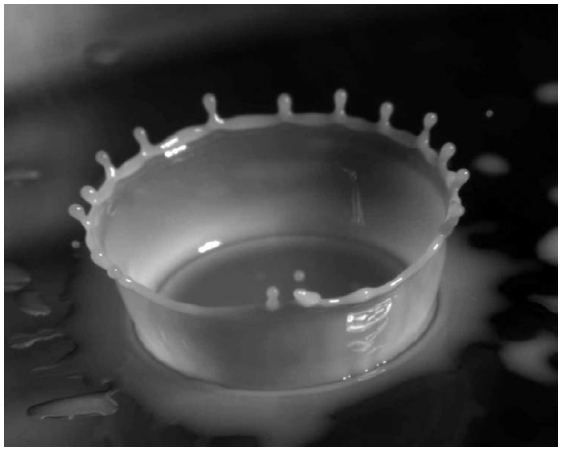

Figure 1.1: Crown splash in milk [57].

and these characteristics are affected by the substrate properties, i.e. wetting and elasticity [25]. The focus of this thesis is to quantify the drop impact dynamics on soft elastic substrates to aide in improving the aforementioned applications.

When a liquid droplet impacts a substrate at high enough velocity secondary droplets can evolve and pinchoff from the primary drop at the leading edge. This is what defines a splash [40]. In applications, such as dentistry, bioprinting, and spray coating, splashing is often not desirable and active splash suppression techniques need to be developed [23]. Xu *et al.* [59] have shown that lowering the air pressure surrounding the substrate decreases the number of satellite drops in a splash and below a threshold pressure no satellite drops are formed at all. Surface chemistry also plays a key role in the characteristics of a splash. The surface roughness and surface chemistry together control the wettability of a substrate [9] and this controls the splashing threshold. It has been shown that drops impacting soft substrates need more that 70% more kinetic energy to splash than on a solid substrate [24].

1.2 Liquid on Liquid Splashing

Drops impacting on liquid layers exhibit numerous different morphologies, as shown in Figure 1.2. Micro-droplets are the first to be observed after impact. The peregrine sheet begins to rise up from the liquid bath and this can turn into a crown splash which can break up into secondary droplets if the initial inertia of the droplet is high enough. As the drop retracts a Rayleigh jet can

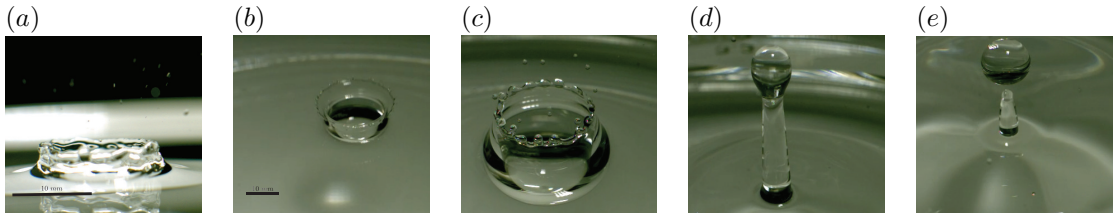

Figure 1.2: Typical splashing morphologies for silicone oil on a liquid bath. (a) Micro-droplets, (b) rising Peregrine sheet, (c) crown splash with droplet breakoff, (d) central jet, (e) central jet breakoff.

form and again if the inertia of the jet is high enough the jet can break up into droplets [8].

The manner in which a droplet splashes during an impact with a liquid surface is reliant on the production of two different sheets. The first being the ejecta sheet, formed at the moment of impact, which was first observed experimentally by Thoroddsen *et al.* [49]. Here a pressure singularity forms at the contact point when the drop impacts the surface which pushes fluid outward. The speed at which the ejecta sheet shoots out has been measured to be as high as 50 m/s [49]. Surface tension can slow the ejecta sheet and Weiss *et al.* [55] showed that for Weber number $We < 40$ no ejecta sheet was produced. It is thought that secondary droplets that appear before a crown splash has formed are due to the breakup of the ejecta sheet [16]. Once the drop has penetrated the fluid layer the peregrine sheet forms. This was first observed by Peregrine *et al.* [37] and is what carries the leading edge or the rim that has the ability to become finger-like which can lead to instability and the formation of secondary droplets. At low impact velocities a thin layer of air can become trapped between the droplet and the liquid bath. This air pocket will breakdown to form a chandelier of bubbles known as Mesler entrainment [44].

Liquid baths can be described as thin or thick depending on the dimensionless fluid thickness, H^* normalized by the droplet diameter [54]. For thin films $H^* \ll 1$, the thin film jets out almost immediately and arises in an impact neck region. At short times the sheet grows rapidly and can become unstable and form fingers. For thick films $H^* \gg 1$, a large cavity forms under the liquid surface and as this cavity fills with liquid a sheet rises upward and can become unstable and form the finger-like structure. Impacts on thin films result in a crown splash that is oriented radially whereas on thick films the crown splash is vertical [29].

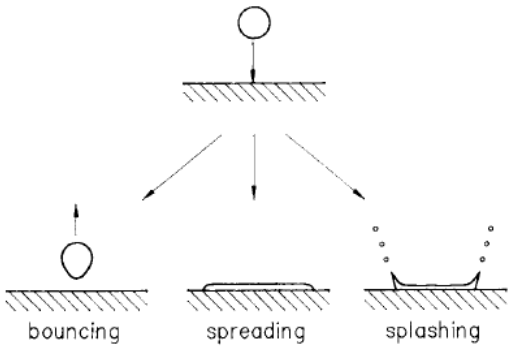

Figure 1.3: Typical drop impact phenomena on solid substrates [38]

1.3 Splashing on rigid substrates

Drop impact on solid substrates exhibit different dynamics with the most common being bouncing, spreading, and splashing [38], as shown in Figure 1.3. These impacts generally depend upon impact velocity, liquid viscosity, and surface wettability. By simply changing the wetting contact angle, Lin *et al.* [28] observed deposition (spreading), partial rebound, full rebound, bubble entrapment on both the surface and the droplet, and splashing.

When a droplet first impacts a solid substrate it is likely to result in a prompt splash [40]. That is, liquid is ejected diagonally away from the contact line between the drop and the solid substrate [58]. These droplets form at the tip of the the lamella at high speeds and is known to happen within 10 μs [53]. The other type of splashing on solid substrates is a corona splash, which is also seen on liquid substrates [58]. The corona splash occurs later during the impact and can be described as droplets forming around the rim of the corona [39]. During a corona splash the lamella, still intact, separates from the solid surface and eventually reaches a bowl shape with droplets ejecting from its finger-like structures [53].

Stow *et al.* [48] developed an empirical relationship for the so-called splash factor $S = rv^{1.69}$, where r is the droplet radius and v is the impact velocity. An impact would result in a splash when this value exceeds a critical splashing threshold constant $S > S*$ [48]. He also showed the normalized watersheet radius, $\alpha = d_{max}/d$ where d_{max} is the watersheet radius and d is the droplet diameter, grew quickly to around 4 times the droplet diameter then shrunk due to surface tension forces as shown in Figure 1.4. By graphing the normalized spreading diameter against the Weber number, all their data collapsed to a power law curve $d_{max} \sim d\, We^{1/4}$ [14]. This scaling was further confirmed by

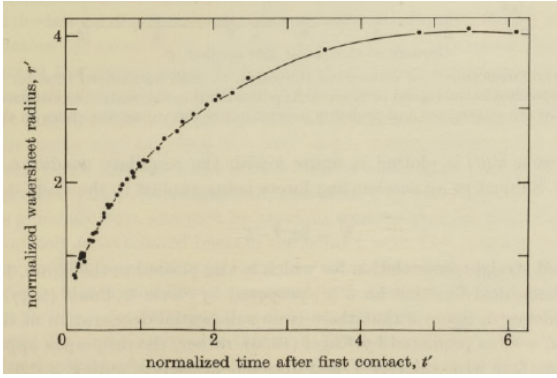

Figure 1.4: Normalized watersheet radius vs. normalized time [48]

other researchers using super-hydrophobic surfaces, partially-wetting surfaces, machined aluminum, and linen paper. Trials were taken on a super-hydrophobic surface, a partially wettable surface, a smooth aluminum plate, and thick linen paper [4]. All of this data fit well to the above scaling relationship. For more viscous liquids they noted that the scaling arguments had to be altered because of the smaller degree of spreading due to the retarding forces of viscosity. The transition from a liquid with a low viscosity to a liquid with a high viscosity impact occurs when the impact factor $P = WeRe^{-4/5} \approx 1$ [14].

Drop spreading and retraction during impact is important in drop deposition technologies and Andrade *et al.* [2] investigated the affect of liquid properties for impact on food substrates including banana and purple cabbage. They found that as the Weber number increased so did the max spreading factor confirming previous work that showed inertia controls the majority of the spreading stage. Their work agreed with [14] and the data for the low viscosity liquids fit the relationship given by $\alpha \sim We^q$ shown where $q = 0.16 \pm 0.02$ for higher viscosity fluids and $q = 0.25 \pm 0.02$ for lower viscosity fluids. A unified model was proposed, $\alpha = 1.28 + 0.071We^{1/4}Re^{1/4}$, that fit the majority of their data. Work has been done to assess the difference between simple and complex surfaces [31]. This theoretical work focused on the flow inside of the lamella and they find that the evolution of the dimensionless thickness of the lamella is a universal function in that it does not depend on impact parameters. This contradicts many early models for droplet impact and only holds when the thickness of the lamella is larger than the thickness of the viscous boundary layer appearing near the substrate directly after impact. Taking into account this boundary layer their equation for the lamella thickness becomes $\bar{h} = \bar{h}_{invisc} + 4/5\gamma Re^{-1/2}$ with $\gamma \approx 0.6$. Furthermore,

they show that one of the more popular ways to predict the maximum spreading factor, using an energy balance, is not correct as it does not account for the edge effects in the lamella. They show good agreement with [14] in the capillary regime with a impact factor less than 1. More recently work has been done to identify the effect of textured surfaces on droplet spreading. This has been done by isolating the spreading factor for perpendicular grooved substrates and parallel grooved substrates. They found that for droplet spreading perpendicular to the grooves there was a critical velocity at which above some of the impacting fluid would impregnate the grooves and while below which no fluid would enter the grooves. They also found that when spreading perpendicularly the front of the droplet would become pinned at the edge of a solid pillar resulting in a smaller max spreading factor compared to the spreading factor parallel to the groves. The difference between the spreading factor perpendicular and parallel to the groves increases with the Weber number. This follows the difference between spreading on a smooth surface versus spreading on a textured surface [51].

1.4 Splashing on soft solids

Investigation into the influence of substrate elasticity on droplet impact was first studied by Rioboo *et al.* [41] who showed that contact angle hysteresis was prominent on elastomer substrates. He showed that the hysteresis was a function of the impact velocity which influences the amount of substrate deformation, demonstrating the effect of substrate deformation on the impact dynamics. Later, Chen *et al.* [11] showed that drops could fully rebound off soft substrates with elasticity $E \sim 4$ kPa. Before this investigation the phenomena of full droplet rebound was seen only on rigid superhydrophobic surfaces. They hypothesize the mechanism of full rebound being the formation of an air film at the interface due to the deformation of the substrate which was later proved by showing the presence of an air film under the rebounding droplet [12].

Substrate elasticity has been shown to provide no effect on the spreading stage of an impacting droplet while greatly affecting the receding phase [1].Carre *et al.* [7] first described the viscoelastic dissipation retarding force that affects the receding phase so greatly. For reference, the maximum surface deformation was observed to be on the order of 10 μm for a substrate with an elasticity around 17 kPa [30]. More recently, a large study of six substrates with $E \sim 0.20 - 510$ kPa has been done to investigate impact phenomena [9]. They show three distinct possibilities after

impact: deposition, bubble entrainment, and partial rebound. Here the dimensionless maximum spreading factor is shown to scale with $\alpha = We^q$ where $q = 0.25 \pm 0.02$.

The first study to determine if soft substrates could absorb impact energy and suppress splashing was done by Howland *et al.* [24]. They investigated gels with elasticity in the range of $5-500$ kPa and showed that impacts on their softest substrates required 70% more kinetic energy to splash than on rigid substrates. This suppression of splashing is explained by the removal of energy from the ejecta sheet not from the bulk of the liquid droplet. With the ejecta sheet having less energy it is harder for it to break up and therefore a prompt splash is avoided. Most recently work has been done to confirm the ability for soft substrates to suppress splashing [19] by controlling the tension of the membrane to 'alter' the elasticity. Here decreasing the substrate elasticity increases the splashing threshold. A new criteria is proposed for splashing that incorporates the substrate elasticity by including the dimensionless time of membrane deformation.

1.5 Thesis Organization

In order to better understand drop impact dynamics on soft substrates, we perform a large number of experiments, varying multiple experimental parameters, and comparing the splash morphology between soft substrates and rigid substrates. Two gel substrates are used in our experiments, PDMS silicone and gelatin hydrogel, and the range of elasticity is $E = 510 - 47,000$Pa. For each liquid/substrate combination, we quantify the splashing threshold. That is, the largest Weber number We for a droplet to fully deposit. During impact, spines are formed at the liquid rim and we quantify how elasticity affects this quantity. Lastly, we show how liquid wetting properties and substrate elasticity affects the ability of a drop to spread and retract during impact. We conclude with some remarks on the applicability of our study in numerous technologies and applications.

Chapter 2

Experiment

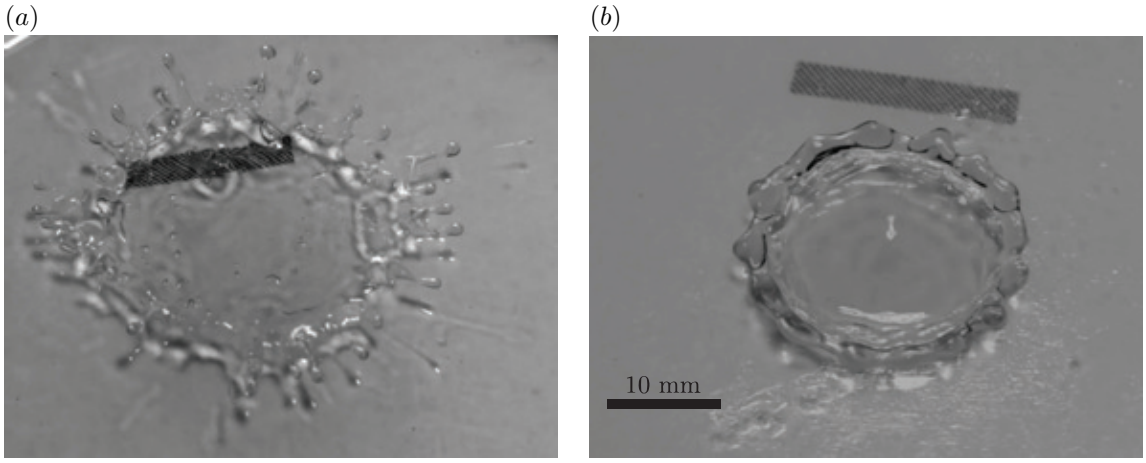

Figure 2.1: Typical drop impact experiment with water on a 7kPa hydrogel showing (a) splashing and (b) deposition.

A liquid drop impacting a solid substrate at a given velocity can either splash or deposit, depending upon the liquid properties and substrate elasticity, as shown in Figure 2.1. We perform drop impact experiments on soft substrates (PDMS silicone gels and gelatin hydrogels), quantifying this dependence on the splash morphology over a large range of experimental parameters.

2.1 Experimental Set-Up

The experimental setup consists of a structural apparatus made of 80/20 aluminum bars, syringe pump and syringe, Phantom high-speed camera, 500 watt LED light source, and substrate holder as shown in Figure 2.2. Drops are formed at the end of a 0.69 mm diameter nozzle that is connected to a NE-1000 syringe pump with slow volumetric flow rate such that the drop volume evolves quasi-statically. For a given nozzle size, drops will break off the nozzle due to surface tension at which point it becomes a falling oblate drop. As the droplet breaks off it oscillates on its fall until it becomes essentially spherical [10]. We verify this by measuring the ratio of the maximum vertical length to the maximum horizontal length for the falling droplets. We note that a perfectly spherical drop would have a ratio equal to 1. For water we measure a ratio of 0.975 and for ethanol we measure a ratio of 0.958 confirming that the drops are essentially spherical. The drop height H varies between $12 - 80$ cm and this results in a range of impact velocities between $1.53 - 3.96$ m/s defined by the free fall velocity $v = \sqrt{2gH}$.

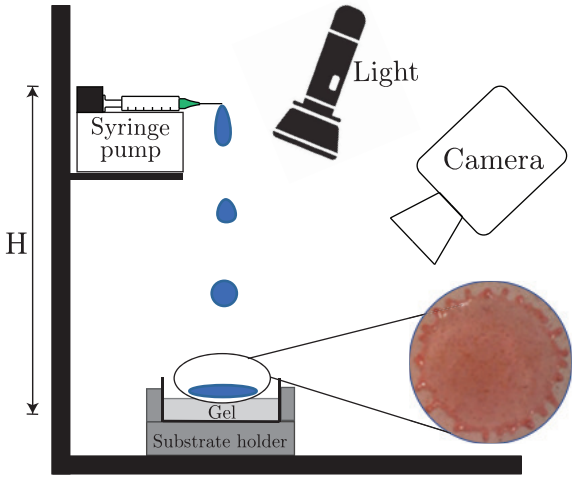

Figure 2.2: Experimental set-up.

Parameter	Range
Nozzle Height (H)	$0.12 - 0.80$ [m]
Drop Velocity (v)	$1.5 - 3.9$ [m/s]
Gel Elasticity (E)	$520 - 47,000$ [Pa]

Table 2.1: Experimental variables

Fluid	Droplet Diameter, d [mm]	Static Contact Angle, θ [deg]
Water	3.6	105 (Gelatin) & 89 (PDMS)
Ethanol	3.2	45 (Gelatin) & 30 (PDMS)

Table 2.2: Liquid droplet properties

Two liquids were used in experiments; i) deionized water and ii) ethanol, and their fluid properties are shown in Table 2.2 & 2.3. Here density ρ was measured with an Anton Paar DMA 35 density meter, viscosity η with an Anton Paar MCR 302 rheometer, and surface tension σ with a Krüss K100 tensiometer with Wilhemly plate. The drop diameter d was 3.6 mm for water and 3.2 mm for ethanol and showed only small variation. This corresponds to a Weber number

$$We = \rho v^2 d/\sigma \tag{2.1}$$

in the range $100 - 1800$ and Reynolds number

$$Re = vd/\eta \tag{2.2}$$

in the range $3500 - 14000$.

Fluid	Viscosity η [mm^2/s]	Density ρ [kg/m^3]	Surface Tension σ [mN/m]
Water	1.0	980	71.6
Ethanol	1.37	760	22.1

Table 2.3: Fluid properties

2.1.1 Gel substrates

Silicone gels (Gelest) are comprised of 3 separate parts; base, cross-linker, and catalyst. To prepare the gel, the base and the catalyst are mixed together in a 99.95%-.05% weight ratio to form part A of the mixture. The base and the cross-linker are combined in a 90%-10% weight ratio to form part B of the mixture. Parts A & B are then mixed together, cast into a container and baked in a IVYX Scientific oven at 63° Celsius for 6 hours. The gels are covered for at least 12 hours. Oscillatory rheology tests are performed on an Anton Paar MCR 302 rheometer to characterize the complex modulus $G = G' + iG''$ where G' is the storage modulus and G'' the loss modulus. A typical

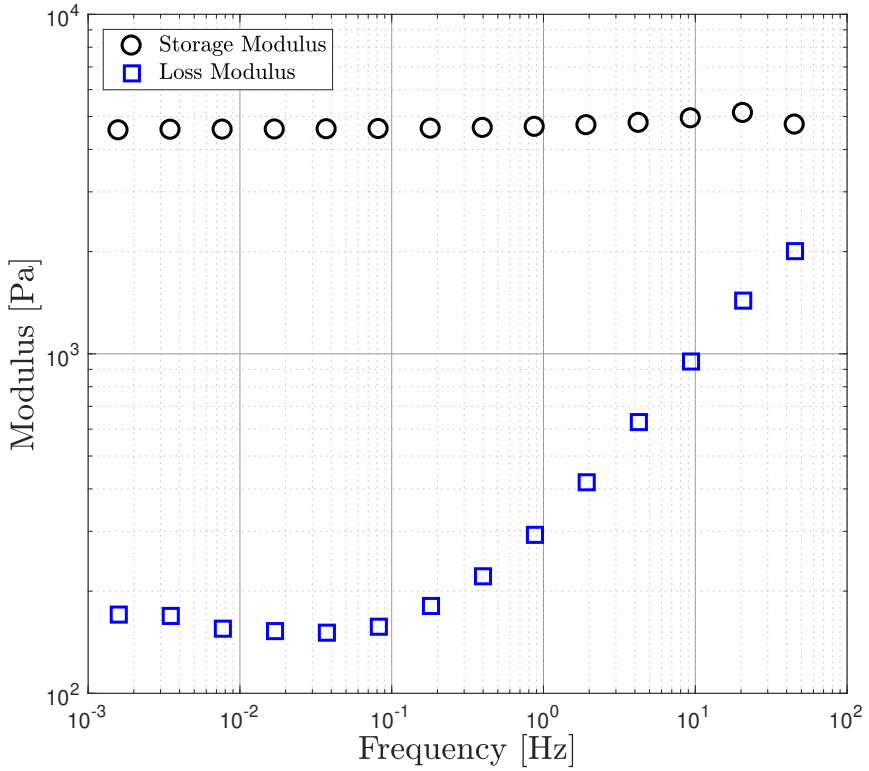

Figure 2.3: Oscillatory rheology test of a typical PDMS gel plotting storage and loss modulus against frequency.

test is shown in Figure 2.3, which plots G', G'' against the frequency. Note that both G' & G'' are constant for low frequency and we use these values to characterize the material. Figure 2.4 shows how the modulus changes with ratio of parts A & B of the mixture. For PDMS silicone gels, the range of shear modulus $G \equiv G'$ is 4.5 to 47.4 kPa.

Gelatin hydrogel substrates are made by dissolving bovine powder (Sigma Aldrich G9382) into deionized water. The gelatin powder used has its strength defined by a 225g Bloom number. These gels are prepared by heating 20 g of water in a beaker on a hot plate at 70° C. Gelatin powder is added to the water and stirred for 60 minutes at which point it is completely dissolved. The mixture is then cast into a container, covered to minimize evaporation, and left to cool overnight. Figure 2.5 plots the storage and loss modulus against the percent weight of gelatin powder. The gelatin hydrogels are all used in experiment within 1 day, after which evaporation starts to alter the material properties of the gel.

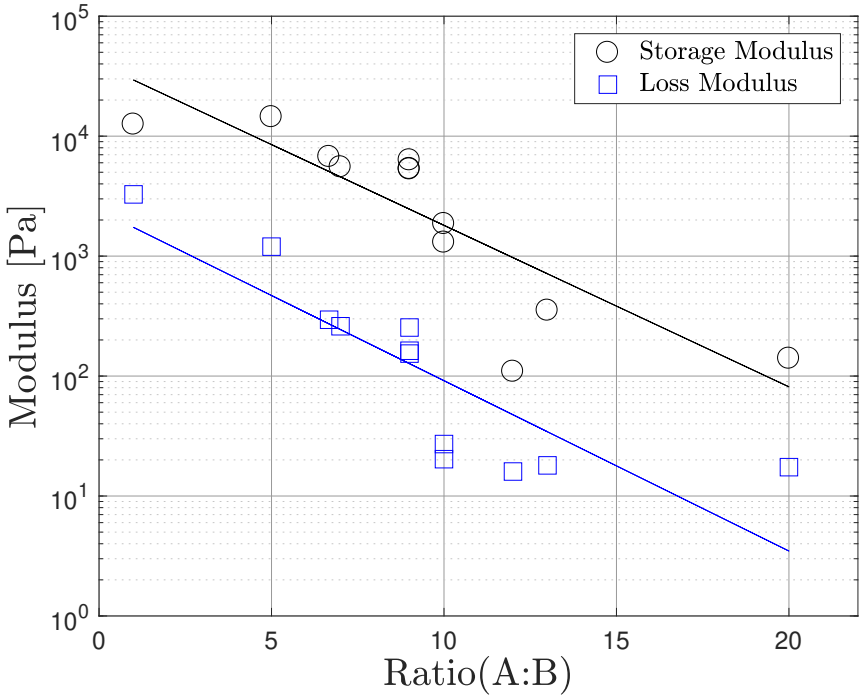

Figure 2.4: Dynamic modulus against ratio of base and catalyst to base and cross-linker for PDMS silicone gels.

Each gel (PDMS and gelatin) is cast into a Petri dish with an inner diameter of 60 mm. The thickness of the gel is 7 mm $\pm$ 2 mm. Both gels are generally incompressible with Poisson ratio $\nu = 1/2$ such that the elastic modulus $E = 2(1+\nu)G$ is $E = 3G$ [56]. The range of elasticities for our silicone gels is $E = 4.5 - 47$ kPa and for our hydrogels is $E = 0.52 - 7$ kPa. We did not use ethanol on our softest hydrogels because this caused the surface to breakdown.

2.2 Protocol

A detailed experimental protocol was followed during these experiments. First, we cast the desired gel into a Petri dish and place it into the substrate holder with scale bar clearly displayed. The LED light source illuminates the center of the substrate. A static drop is placed on the substrate and the camera is focused. This is done because of the small depth of field. Liquid is mixed with red food coloring in a ratio of 100 ml to 5 μL. It is then loaded into a syringe and placed in the syringe pump at the desired height above the substrate. A low flow rate then generates drops. Drop

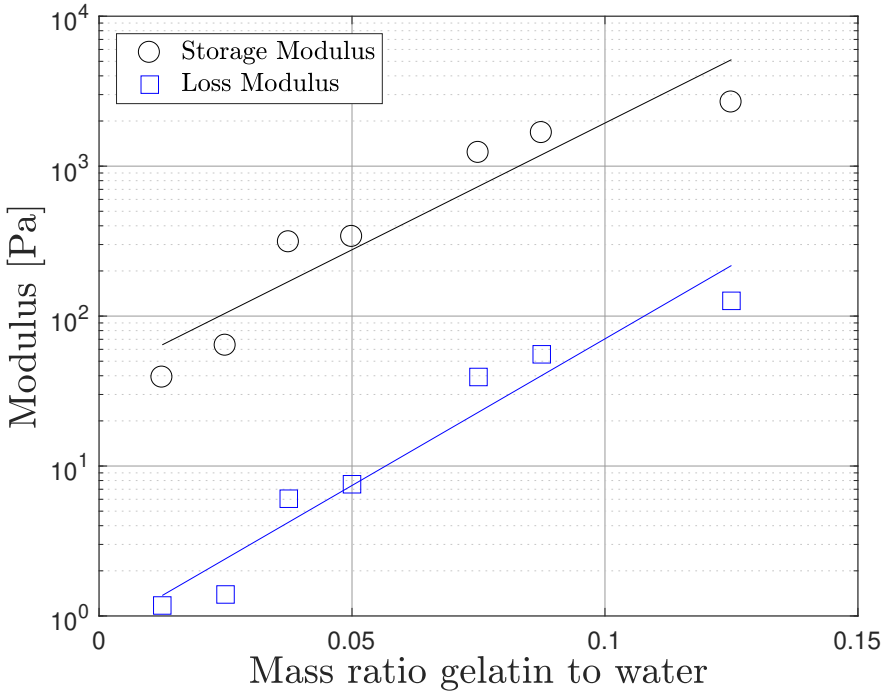

Figure 2.5: Storage and loss modulus as it depends upon the mass ratio of gelatin powder.

impact is captured by the camera at 5200fps. After each drop impact, the substrate is dried with a laboratory tissue. Each experiment is repeated 5 times. Great care was taken to make sure the experiments were accurate and repeatable.

2.3 Image processing

For each experiment, the drop impact is recorded with high-speed camera. A predetermined bar was included in each image used to calibrate the length measurements. Figure 2.6 shows a typical experiment in which a drop of diameter d impacts a substrate, spreads to a maximum diameter d_{max}, and then retracts to its final diameter d_{final}. High-speed video from each experiment is used to extract d_{max}, d_{final}, and the spine number N during a splash event. The spine number N is illustrated in Figure 2.7. Note that $N = 0$ corresponds to the absence of any spines in an almost perfectly circular spread. Each video is processed in Adobe Premiere Pro and the individual frames are identified to find d_{max} and d_{final}. ImageJ is used to quantify d_{max}, d_{final} and N, with lengths correlated to a known value in the image. These define the splash morphology. We define the

spreading factor as the ratio between the maximum spread diameter of the impacting droplet and the initial diameter of the droplet given by $\alpha = d_{max}/d$ and retraction factor defined as the final diameter of the impacting drop divided by the initial drop diameter given by $\beta = d_{final}/d$. We will use these two quantities α, β to normalize and report our results.

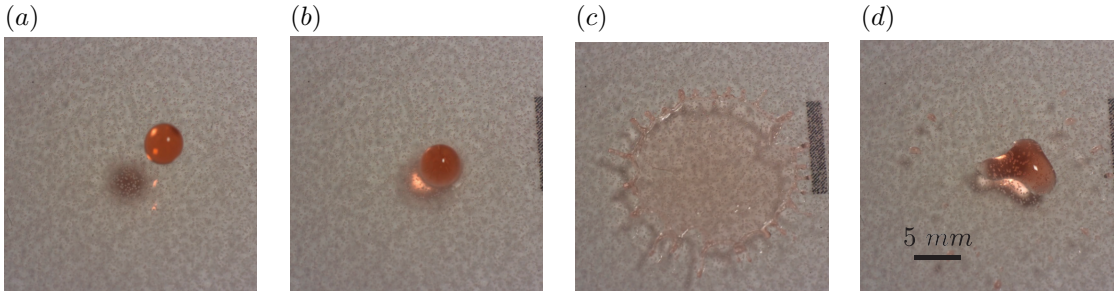

Figure 2.6: Definition of spreading factor α and retraction factor β. A drop of diameter d impacts a substrate and spreads to a maximum diameter d_{max} and then retracts to a final diameter d_{final}.

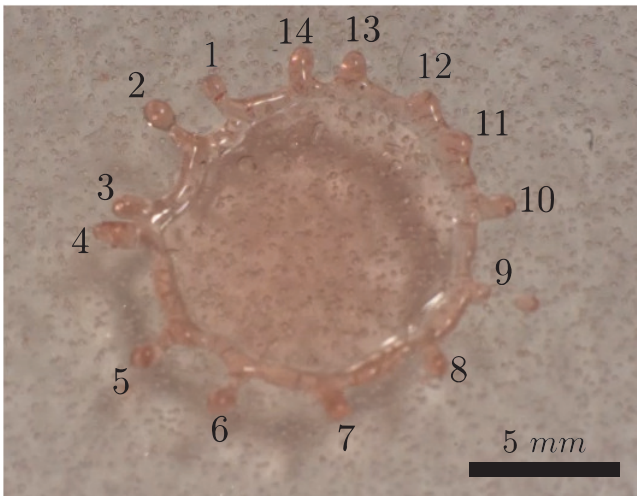

Figure 2.7: Experimental image showing spine number N

Chapter 3

Results

In this section, we experimentally quantify the splashing threshold, spreading factor, retraction factor, and spine number, as they depend upon the liquid properties, drop velocity, and substrate elasticity. The focus is on soft substrates, but for reference we use acrylic as a proxy for what we will refer to as a 'hard substrate' with an elasticity much greater than the gels used in our experiments. The other extreme is the limiting case of a substrate with no elasticity, i.e. a liquid, and we include those results in Appendix A.

3.1 Splashing

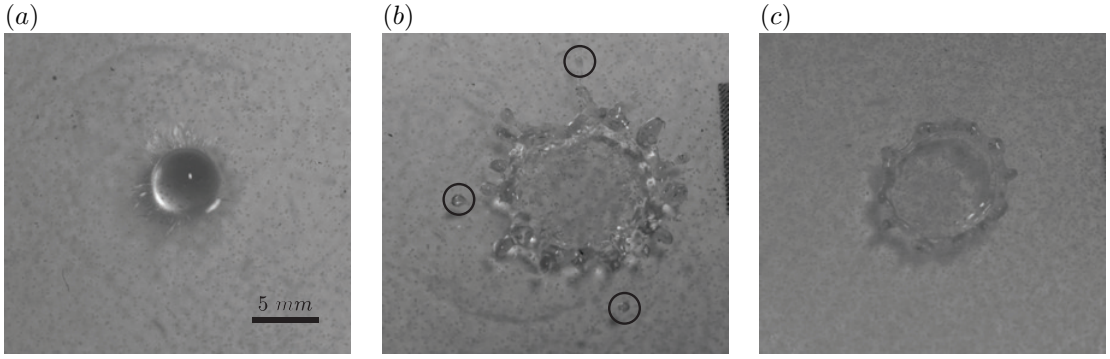

Figure 3.1: Drop impact can lead to either (a) micro-droplet splash, (b) secondary droplet splash, or (c) deposition.

During a given experiment, the simplest observation is whether the drop i) splashes or ii)

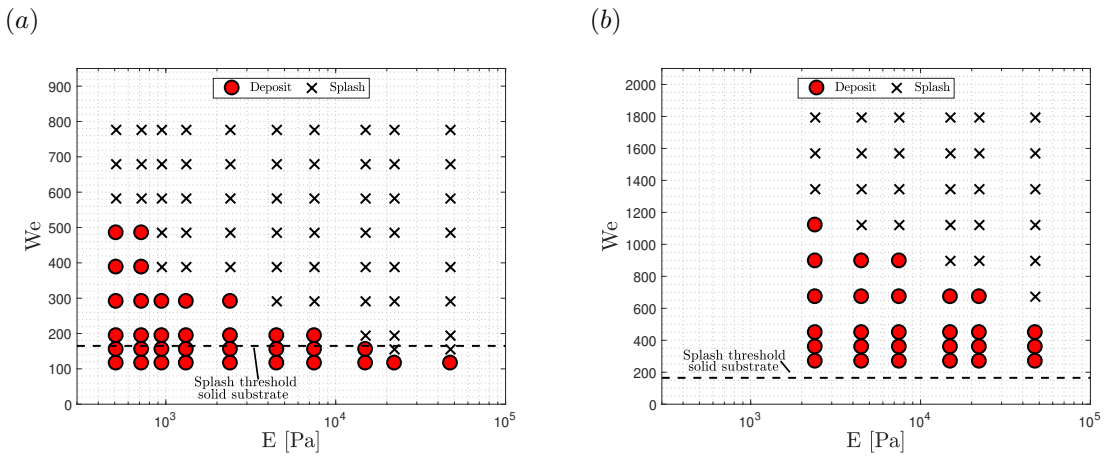

Figure 3.2: Phase diagram plotting the Weber number We against the substrate elasticity E for (a) water and (b) ethanol showing regions of drop deposition and splashing. Note the different y-axis scales in the subplots.

deposits on the substrate. This distinction is important in many inkjet printing applications as splashing is undesirable from a quality control perspective. We define a 'splash' as either i) a drop that produces micro-droplets immediately after impact or ii) a droplet that exhibits two or more satellite drops that break off from the fingers that extend off of the main drop during impact. This distinction is shown in Figure 3.1 which contrasts three impacts which result in a (a) micro-droplet splash, (b) secondary droplet splash, and (c) deposition. Note in figure 3.1 (b) the small secondary drops that have broken off at the tips of the finger-like spines. Splashing typically occurs when the liquid inertia overcomes the surface tension forces.

As such, splashing is typically quantified by the Weber number We. On soft substrates, one might expect that some of the liquid energy can be transmitted into the elastic energy of substrate deformation, therefore affecting the impact dynamics and the ability to splash. This is illustrated in the phase diagrams shown in Figure 3.2 which plot the Weber number We against the substrate elasticity E and define regions of splashing and deposition. For a fixed elasticity E, splashing occurs at larger Weber numbers indicative of the higher inertia required to produce a splash. For softer substrates (lower E), a higher We is required to produce a splash, indicating that it is harder to splash on soft substrates. Note that each marker is an average of five trials, as such the closer to the splashing threshold the more statistical uncertainty. The dashed line in Figure 3.2 denotes the splash threshold for hard substrates [24]. Our data respects this bound and we have independently verified it using an acrylic substrate with elasticity $E \approx 3.2$ GPa. Even though the phase diagrams

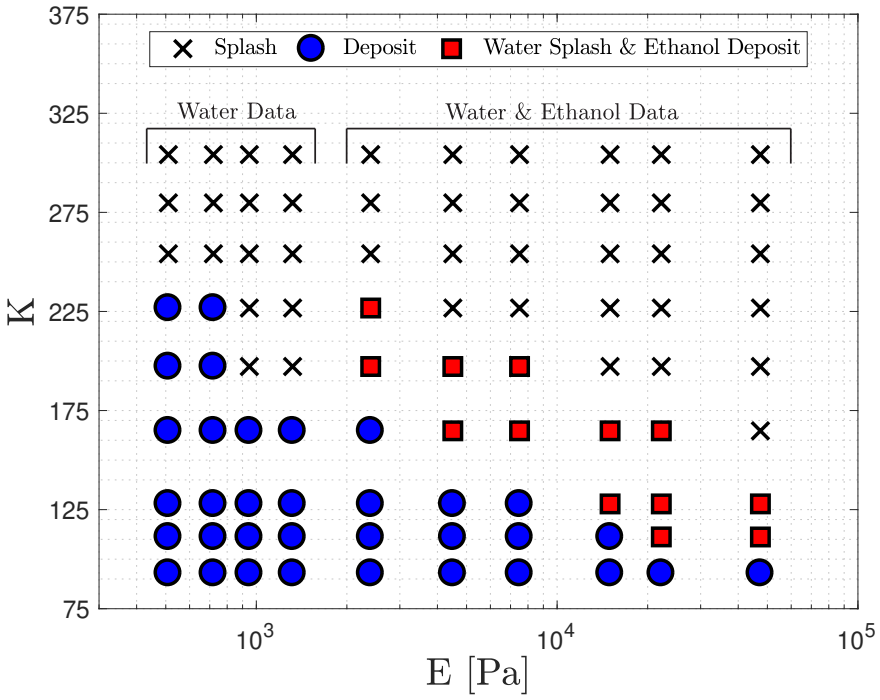

Figure 3.3: Combined phase diagram plotting the nondimensional parameter $K = Re^{1/4} * We^{1/2}$ against elasticity E showing regions of splashing, deposition, and an overlap region where water splashes but ethanol deposits.

for water and ethanol appear qualitatively similar, they are not quantitatively similar as evident by the difference in vertical scale. Work by Mundo *et al.* [34] have suggested the dimensionless number $K = Re^{1/4} * We^{1/2}$ as an effective metric to quantify splashing. We attempt to collapse all of our data in the phase diagram of Figure 3.3, which plots K against E. The collapse is reasonable with the exception of the small overlap region where water splashes and ethanol deposits.

3.2 Spine Number

Splashes and depositions are typically preceded by the formation of spines off the rim of the spreading drop, as shown in Figure 3.1. Figure 3.4 plots the spine number N against Weber number We for (a) water and (b) ethanol. For water, the spine number N increases with substrate elasticity E for all Re, with the largest spine number occurring for the acrylic substrate ($E = 3.2$ GPa) and smallest spine number for our softest hydrogel ($E = 510$ Pa). For ethanol, the trend is opposite that

of water with the lowest spine number corresponding to the acrylic substrate.

(a)

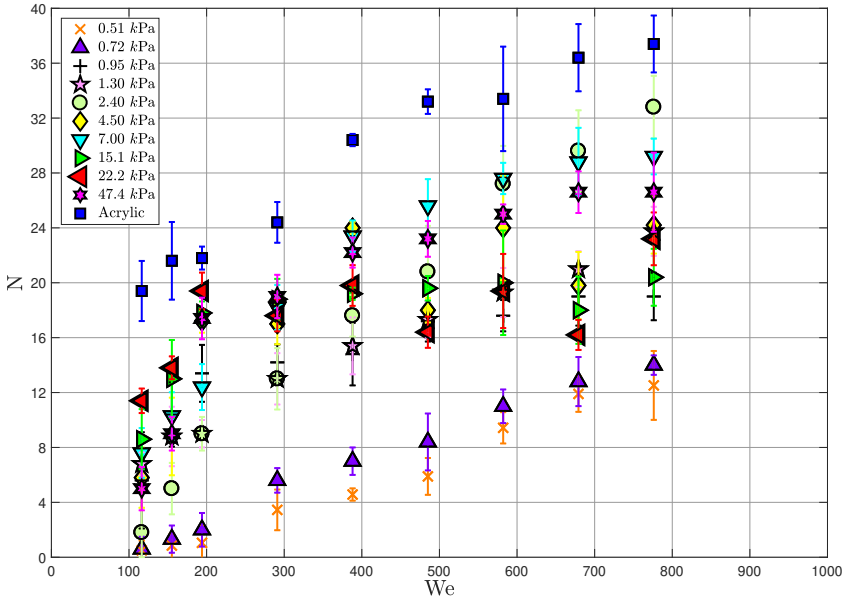

(b)

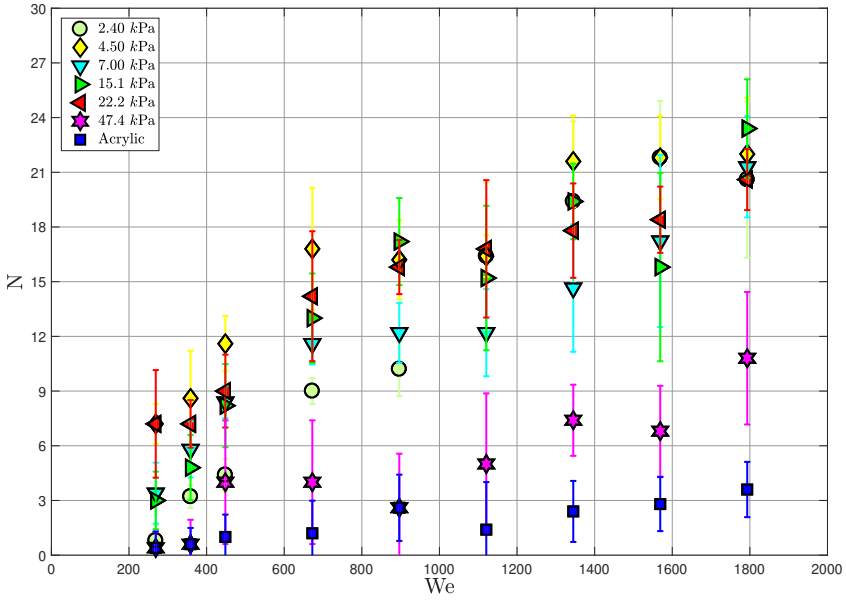

Figure 3.4: Spine number N against Weber number We for (a) water and (b) ethanol. Error bars are 95% confidence intervals.

We attribute this observation to the inherent difference in wetting effects between water and ethanol. Typical drop shapes with spines are illustrated in Figure 3.5, as it depends upon the impact velocity. In general, increased impact velocity leads to a higher spine number but also greater disorder in the spatial distribution of the spines along the drop periphery.

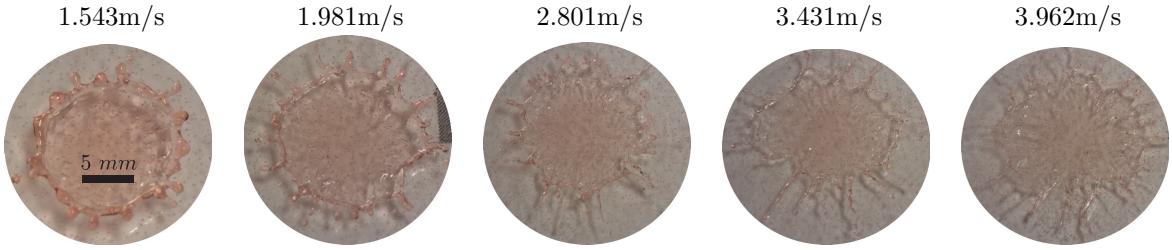

Figure 3.5: Contrasting the spine number N as it depends upon the impact velocity v for water. The substrate is PDMS silicone with $E = 22$kPa.

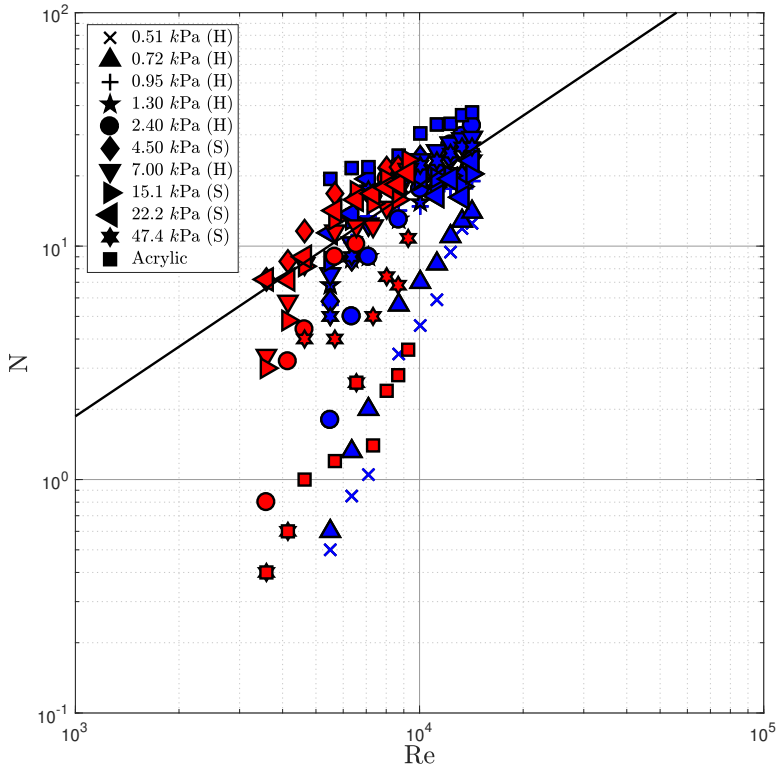

Figure 3.6: Spine number N against Reynolds number Re for all data, blue is water and red is ethanol. The trend line is the best fit line $N \sim Re$. Note each data point is the mean of 5 tests.

In Figure 3.4, note that for fixed elasticity the trend with Re appears to be linear for all but a few data sets. This is clear in Figure 3.6 which plots all of our data that collapses to the power law curve $N \sim Re$. This shows reasonable agreement with previous literature; Maramanis *et al.* [32] predicted a scaling of $K^{*3/4}$ where $K^* = Re^{1/2} * We^{1/4}$. We note that our data collapsed much better when taking into account only the Reynolds number Re. The most striking feature is that the water data for our softest gels $E = 510$ & 720 Pa and the ethanol data for our stiffest substrates $E = 47.4$ kPa & 3.2 GPa does not collapse indicating a dependence on the substrate elasticity.

3.3 Spreading Factor

Figure 3.7 plots the spreading factor α against the Weber number We showing an increasing trend with We. For water, the softest gel 510 Pa has the lowest spreading factor and the stiffest substrate acrylic with $E = 3.2$ GPa has the highest spreading factor, indicating that soft substrates inhibit the droplet spreading after impact. This is contrary to previous literature that shows substrate elasticity has very little effect on the spreading factor for droplet impact [26]. Although it has been shown that soft substrates allow small deformations during droplet impact, it has been postulated that these deformations are small enough such that the elastic energy of deformation does not affect spreading or splashing [24]. Our experiments include significantly softer gels which have associated larger deformations that can affect the spreading factor. For ethanol, the data follows the same general trend as water with the stiffest substrate yielding the largest spreading factor. It is also shown that data for hydrogels and silicone gel tend to cluster together. Interestingly, this is not the case for water and we attribute this observation to wetting effects.

Figure 3.8 plots the spreading factor for all of our data against the Weber number We. In general, our data collapses well with the exception the softest substrates. For water, the data collapses to the scaling given by $\alpha \sim We^{1/4}$ which agrees well with [42]. For ethanol, the best fit to the data is $\alpha \sim We^{1/10}$; however, the spread around the fit is large.

3.4 Retraction Factor

Following spreading, the drop retracts from its maximum diameter due to surface tension effects and equilibrates at its final diameter. We plot the retraction factor β against the Weber

number We for (a) water and (b) ethanol in Figure 3.9. For water, the general trend is that the retraction factor increases for softer substrates. This agrees well with the literature in which the final diameter increases with decreasing stiffness [1]. There is a clear distinction between the hydrogel and silicone gel substrates; silicone gels have lower β meaning they retract more than the hydrogels. The acrylic substrate data falls between that for hydrogels and the silicone gels.

Previously it has been shown that the softness of deformable substrates absorbs the energy of impact and the drop cannot retract back. This is attributed to substrate deformation at the three-phase contact line. The substrate deformation provides additional dissipation to the contact line motion which reduces the velocity of the receding droplet [26]. The ethanol data is harder to interpret. As with water, the hydrogel and silicone gels appear to have their own regimes with the exception of the stiffest silicone gel 47 kPa. Most interestingly we report the highest retraction factors for water are seen on our hydrogels with the highest being on our 7 kPa substrate. For ethanol, however, we see our highest retraction factors on the silicone gels with the highest on our stiffest substrate, acrylic. This difference is presumably due to the wetting effects for the different liquids. A more detailed study of the retraction dynamics could be pursued to test this hypothesis.

(a)

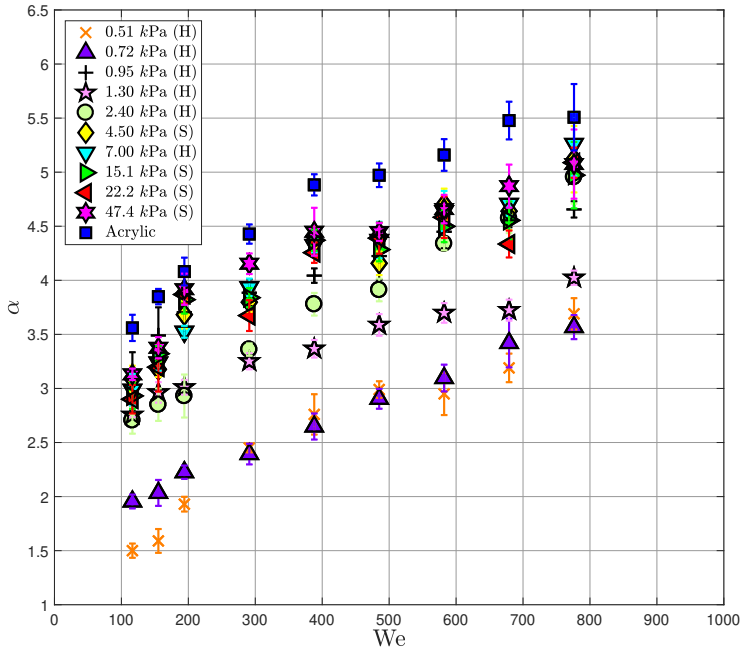

(b)

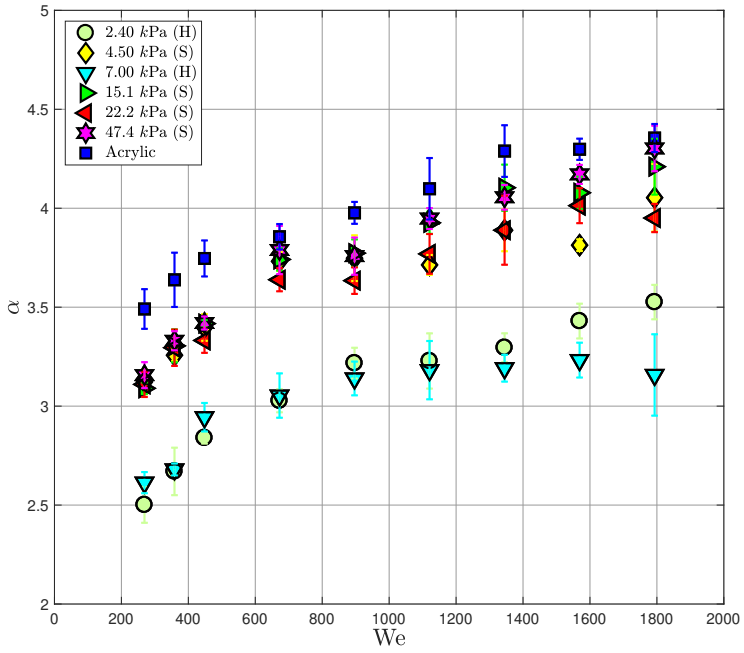

Figure 3.7: Spreading factor α against Reynolds number Re for (a) water and (b) ethanol.

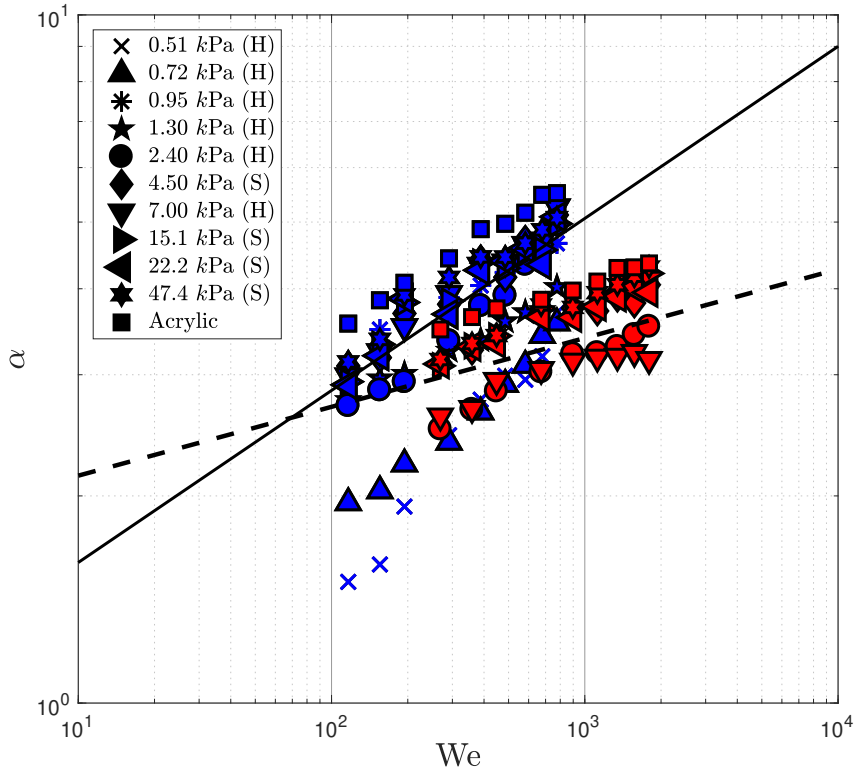

Figure 3.8: Spreading factor α against Weber number We for all data. Solid trendline is $\alpha \sim We^{1/4}$. Dashed trendline correspond to $\alpha \sim We^{1/10}$.

(a)

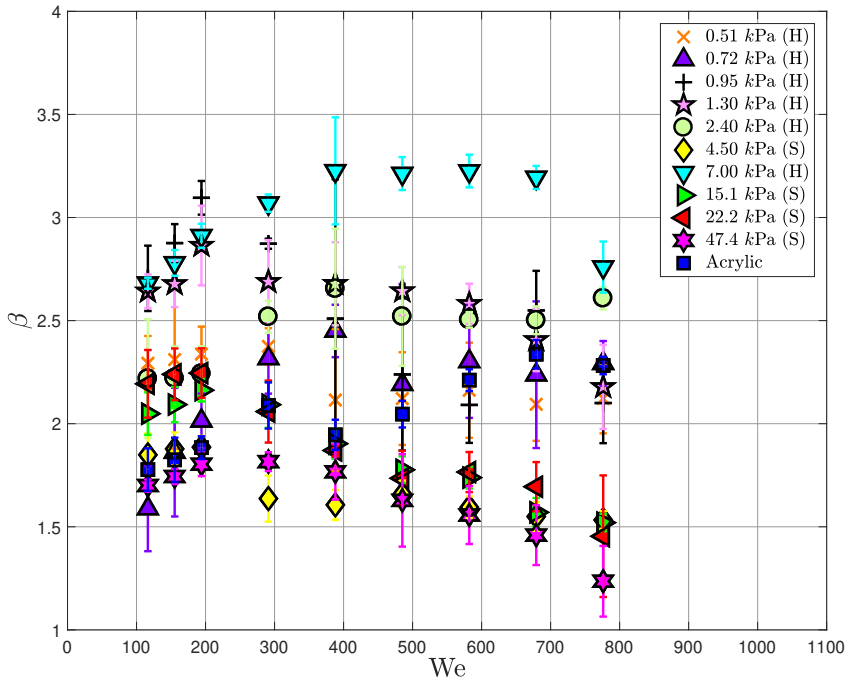

(b)

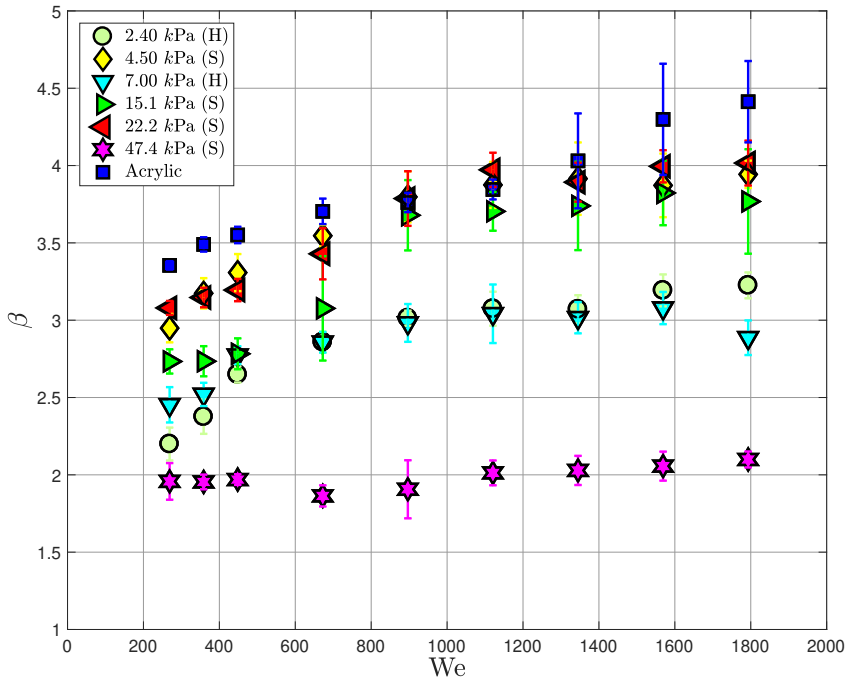

Figure 3.9: Retraction factor β against Weber number We for (a) water and (b) ethanol.

Chapter 4

Discussion

We have experimentally quantified the drop impact dynamics on soft substrates. The splashing threshold, as described by the Weber number, is important for quality control purposes in inkjet printing applications and bioprinting technologies in particular [52]. Our results agree well with Howland *et al.* [24] in that soft substrates have a much higher splashing threshold than stiffer substrates and we have quantified this for multiple liquids and multiple gel substrates. Our work is distinguished in that we explore much softer gels with elasticity as low as $E = 510$Pa. This is approaching a lower bound for our splashing experiments, as it is well known that drops can cause starburst fractures on ultrasoft gels ($E \approx 50$Pa) [15, 46, 6, 21]. For a given substrate, ethanol consistently displays a higher splashing threshold relative to water, which we attribute to increased viscosity that slows the eject sheet thus suppressing splashing.

The spine number is shown to correlate with the Reynolds number, $N \sim Re$ and this is in decent agreement with Marmanis *et al.* [32] who show $N \sim (We^{1/2} * Re^{1/4})^{3/4}$. Interestingly, our data for water on the softest substrates and ethanol on our hardest substrates does not collapse upon this scaling, leading us to believe that an essential piece of physics is missing and this may include wetting or viscoelastic effects due to the substrate.

The spreading factor α is an important criteria in applications such as aerosol drug delivery, ink jet printing, and bio printing [25, 50, 52]. Figure 3.8 plots all of our data for the spreading factor against Weber number and we show two distinct trends; i) for water $\alpha \sim We^{1/4}$ and ii) for ethanol $\alpha \sim We^{1/10}$. These conflicting trends are presumably due to the differing liquid properties of each. Similarly, the data does not collapse for either liquid on our softest substrates indicating

that elasticity plays a role in governing the spreading dynamics. Despite these discrepancies, we do show very good agreement with Andrade *et al.* [2] who show that for low viscosity liquids the spreading factor scales by $\alpha \sim We^{0.25\pm0.02}$ and for higher viscosity liquids the spreading factor scales by $\alpha \sim We^{0.16\pm0.02}$. Our data shows good agreement with this scaling shown in Figure 3.8 where we scale the spreading factor for water by $\alpha \sim We^{0.25}$ and the spreading factor for ethanol scales with $\alpha \sim We^{0.10}$. These scaling power laws are within the error bounds for our results.

The retraction factor β has data that is more skewed than the other experimental output. Our water data provides rough agreement with Alizadeh *et al.* [1] who shows that for decreasing substrate stiffness a decreased drop retraction is observed. Interestingly, we show that for water the retraction factor is relatively unaffected by the Weber number, as shown by the flat curves in Figure 3.9 (a). The data for the ethanol drops deviates significantly from [1], by showing that there is no discernible relationship between the substrate elasticity and the retraction factor. We believe this discrepancy to be caused by the wetting effects.

Throughout this work we have shown that substrate elasticity affects the impact dynamics. We believe that along with substrate elasticity we also expect the liquid/substrate wettability to play a large role in how droplets create spines, spread to a maximum diameter, and retract to an equilibrium shape. Previous literature has shown that when comparing substrates, high wettability favors liquid displacement and the suppression of spine number in spreading droplets [17]. We see this phenomena in Fig 3.6 which plots the combined spine number data against the Weber number. Here we show that for each liquid a much lower number of spines for the substrate with the highest wettability is observed. We believe that the difference in contact angles between our gelatin hydrogels and our PDMS silicone gels explain the grouping of the ethanol data sets seen in Fig 3.7 (b). Although it has not been proven yet we attribute the data with the lowest amount of spreading to be caused by the higher amount of wetting of the ethanol droplets on the hydrogels. Most influenced by the wettability is the retraction phase of the droplet. Bayer *et al.* has shown that wettable surfaces see only slight retraction when compared to surfaces with lower amounts of wettability [3]. This is due to two main effects. First, the smaller contact angle causes lower retraction speeds, consistent with dynamic wetting effects [20, 43, 5]. Second the wettability of the surface has been shown to pin the spreading droplet thus reducing the retraction phase significantly on highly wettable substrates [47]. It has been shown that wettability plays a large role in the impact dynamics of liquid drops on hard solids. Our results on soft solids exhibit similar physics and should be explored further.

Chapter 5

Concluding Remarks

We have performed an experimental investigation into droplet impact on soft substrates, quantifying the splashing morphology by the spine number N, spreading factor α, and retraction factor β. Approximately 1000 experiments were conducted varying impact velocity, substrate elasticity, and fluid properties (η, ρ, γ). High-speed photography and image processing techniques were used to quantify the impact dynamics. Great care was taken to ensure our results were repeatable. We report new splashing thresholds for multiple soft elastic substrates and various liquids. We have shown that for very soft gels we observe significantly different results in both spine number and spreading factor leading us to believe that at very low elasticities different dynamics occur. Lastly we show that the retraction data is unusual and does not have a clear dependence on the substrate elasticity.

Our work can provide new insights into applications and technologies, such as bioprinting, aerosol drug delivery, crime scene investigation, and pesticide application on plants. For example, Figure 3.2 presents a phase diagram to quantify the splashing threshold which can predict the highest drop impact velocity for deposition for a substrate with a given elasticity. This is useful for quality control purposes in tissue engineering applications which involve drop deposition onto soft substrates and also for optimization of the bioprinting process. Lai *et al.* [27] has previously shown that lung elasticity is dependent on the age of the person. It may be possible with our study to customize inhalers in order to maximize the delivery of costly medicines into the lungs. By quantifying the relationship between impact Weber number We and spine number N on elastic substrates we have improved the ability of forensic scientists to backout the impact velocity of drops in blood splat

patterns to better recreate crime scenes. Lastly, there is a critical need in the agricultural industry to be able to efficiently spread and cover the surface area of plants with pesticides or fertilizers and these are often delivered by spray processes. By quantifying the relationship between the spreading factor α and the elasticity E we can determine the optimal impact velocity for pesticide application on a given plant to cover the leaves with the least amount of waste.

To advance this work we would like to measure the advancing and receding contact angles to better understand the difference between the wetting affects of our two types of substrates as we believe these play an important role in the impact dynamics. We are also interested in the contact angle's dependence on substrate elasticity. We believe this could of importance in understanding how substrate elasticity effects impact dynamics. The contact angle measurements could provide an important piece to improve the theoretical models. With better models we can improve the scaling analysis and expect the data to collapse more. Data that is more collapsed leads to better prediction for the impact dynamics that can improve the applicability in the aforementioned applications. We would also like to extend the data set to test softer substrates as this is where the data deviates the most. We also could fill in some of the gaps we have between elasticity's to further confirm the results we have seen. Lastly we would like to test more liquids to better observe the effect the liquid properties (η, ρ, γ) have on impact dynamics.

Appendices

Appendix A Liquid Substrate

Liquids splashing on a bath of the same liquid are a limiting case of a substrate with no elasticity. We conducted experiments into the splash morphology with four different liquids; water, ethanol, 10cSt silcone oil, and 100cSt silicone oil. Figure 1 shows four common liquid on liquid impact phenomena: (a) shows a rising peregrine sheet, (b) a crown formation, (c) micro-droplets breaking off of the crown, and (d) a Rayleigh jet. Figure 2 plots a phase diagram for each respective morphology in the $We - Re$ parameter space. We denote a positive observation by a blue marker and no observation by a red marker. The different liquids are denoted in the legend. We show good agreement with the results of Deegan *et al.* [16].

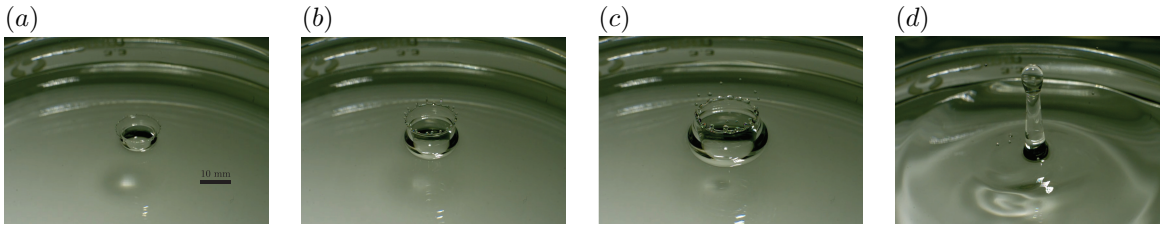

Figure 1: Liquid splashing on a bath of the same liquid exhibits (a) rising peregrine sheet, (b) crown formation, (c micro-droplets breaking off of the crown, and (d) Rayleigh jet.

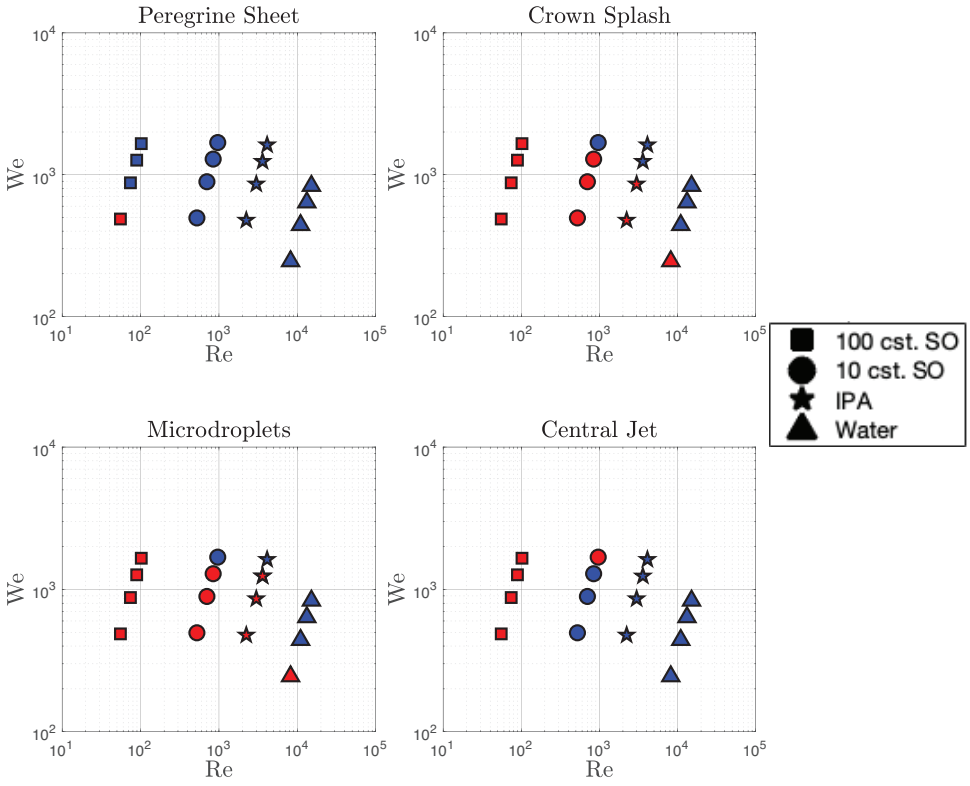

Figure 2: Phase diagram plotting Weber number We against Reynolds number Re for peregrine sheet, crown splash, micro-droplets, and central jet morphologies in liquid splashing on a bath of the same liquid. Liquids used were silicone oils of varying viscosity, isopropyl alcohol, and deionized water.

Bibliography

[1] Azar Alizadeh, Vaibhav Bahadur, Wen Shang, Yun Zhu, Donald Buckley, Ali Dhinojwala, and Manohar Sohal. Influence of substrate elasticity on droplet impact dynamics. *Langmuir*, 29(14):4520–4524, 2013.

[2] R Andrade, O Skurtys, and F Osorio. Experimental study of drop impacts and spreading on epicarps: effect of fluid properties. *Journal of Food Engineering*, 109(3):430–437, 2012.

[3] Ilker S Bayer and Constantine M Megaridis. Contact angle dynamics in droplets impacting on flat surfaces with different wetting characteristics. *Journal of Fluid Mechanics*, 558:415, 2006.

[4] Anne-Laure Biance, Christophe Clanet, and David Quéré. First steps in the spreading of a liquid droplet. *Physical Review E*, 69(1):016301, 2004.

[5] JB Bostwick. Spreading and bistability of droplets on differentially heated substrates. *Journal of Fluid Mechanics*, 725:566–587, 2013.

[6] Joshua B Bostwick and Karen E Daniels. Capillary fracture of soft gels. *Physical Review E*, 88(4):042410, 2013.

[7] Alain Carré, Jean-Claude Gastel, and Martin ER Shanahan. Viscoelastic effects in the spreading of liquids. *Nature*, 379(6564):432–434, 1996.

[8] Eduardo Castillo-Orozco, Ashkan Davanlou, Pretam K Choudhury, and Ranganathan Kumar. Droplet impact on deep liquid pools: Rayleigh jet to formation of secondary droplets. *Physical Review E*, 92(5):053022, 2015.

[9] Longquan Chen, Elmar Bonaccurso, Peigang Deng, and Haibo Zhang. Droplet impact on soft viscoelastic surfaces. *Physical Review E*, 94(6):063117, 2016.

[10] Longquan Chen, Elmar Bonaccurso, and Martin ER Shanahan. Inertial to viscoelastic transition in early drop spreading on soft surfaces. *Langmuir*, 29(6):1893–1898, 2013.

[11] Longquan Chen and Zhigang Li. Bouncing droplets on nonsuperhydrophobic surfaces. *Physical Review E*, 82(1):016308, 2010.

[12] Longquan Chen, Jun Wu, Zhigang Li, and Shuhuai Yao. Evolution of entrapped air under bouncing droplets on viscoelastic surfaces. *Colloids and Surfaces A: Physicochemical and Engineering Aspects*, 384(1-3):726–732, 2011.

[13] YS Cheng, H Irshad, P Kuehl, TD Holmes, R Sherwood, and CH Hobbs. Lung deposition of droplet aerosols in monkeys. *Inhalation toxicology*, 20(11):1029–1036, 2008.

[14] Christophe Clanet, Cédric Béguin, Denis Richard, and David Quéré. Maximal deformation of an impacting drop. *Journal of Fluid Mechanics*, 517:199–208, 2004.

[15] Karen E Daniels, Shomeek Mukhopadhyay, Paul J Houseworth, and Robert P Behringer. Instabilities in droplets spreading on gels. *Physical review letters*, 99(12):124501, 2007.

[16] RD Deegan, P Brunet, and J Eggers. Complexities of splashing. *Nonlinearity*, 21(1):C1, 2007.

[17] Bo Dong, YY Yan, and WZ Li. Lbm simulation of viscous fingering phenomenon in immiscible displacement of two fluids in porous media. *Transport in porous media*, 88(2):293–314, 2011.

[18] Jun Fukai, Y Shiiba, T Yamamoto, O Miyatake, D Poulikakos, Constantine M Megaridis, and Z Zhao. Wetting effects on the spreading of a liquid droplet colliding with a flat surface: experiment and modeling. *Physics of fluids*, 7(2):236–247, 1995.

[19] Marise V Gielen, Riëlle de Ruiter, Jacco H Snoeijer, and Hanneke Gelderblom. Supressed splashing on elastic membranes. *arXiv preprint arXiv:1711.05634*, 2017.

[20] Harvey P Greenspan. On the motion of a small viscous droplet that wets a surface. *Journal of Fluid Mechanics*, 84(1):125–143, 1978.

[21] Marion Grzelka, Joshua B Bostwick, and Karen E Daniels. Capillary fracture of ultrasoft gels: variability and delayed nucleation. *Soft matter*, 13(16):2962–2966, 2017.

[22] Hemanth Gudapati, Madhuri Dey, and Ibrahim Ozbolat. A comprehensive review on droplet-based bioprinting: past, present and future. *Biomaterials*, 102:20–42, 2016.

[23] Stephen K Harrel and John Molinari. Aerosols and splatter in dentistry: a brief review of the literature and infection control implications. *The Journal of the American Dental Association*, 135(4):429–437, 2004.

[24] Christopher J Howland, Arnaud Antkowiak, J Rafael Castrejón-Pita, Sam D Howison, James M Oliver, Robert W Style, and Alfonso A Castrejón-Pita. It's harder to splash on soft solids. *Physical review letters*, 117(18):184502, 2016.

[25] Lee Hulse-Smith and Mike Illes. A blind trial evaluation of a crime scene methodology for deducing impact velocity and droplet size from circular bloodstains. *Journal of forensic sciences*, 52(1):65–69, 2007.

[26] Hannah M Kittel, Ehsanul Alam, Ilia V Roisman, Cameron Tropea, and Tatiana Gambaryan-Roisman. Splashing of a newtonian drop impacted onto a solid substrate coated by a thin soft layer. *Colloids and Surfaces A: Physicochemical and Engineering Aspects*, 553:89–96, 2018.

[27] Stephen J Lai-Fook and Robert E Hyatt. Effects of age on elastic moduli of human lungs. *Journal of applied physiology*, 89(1):163–168, 2000.

[28] Shiji Lin, Binyu Zhao, Song Zou, Jianwei Guo, Zheng Wei, and Longquan Chen. Impact of viscous droplets on different wettable surfaces: Impact phenomena, the maximum spreading factor, spreading time and post-impact oscillation. *Journal of colloid and interface science*, 516:86–97, 2018.

[29] WC Macklin and GJ Metaxas. Splashing of drops on liquid layers. *Journal of applied physics*, 47(9):3963–3970, 1976.

[30] Simone Mangili, Carlo Antonini, Marco Marengo, and Alidad Amirfazli. Understanding the drop impact phenomenon on soft pdms substrates. *Soft Matter*, 8(39):10045–10054, 2012.

[31] Marco Marengo, Carlo Antonini, Ilia V Roisman, and Cameron Tropea. Drop collisions with simple and complex surfaces. *Current Opinion in Colloid & Interface Science*, 16(4):292–302, 2011.

[32] H Marmanis and ST Thoroddsen. Scaling of the fingering pattern of an impacting drop. *Physics of fluids*, 8(6):1344–1346, 1996.

[33] A Mongruel, V Daru, F Feuillebois, and S Tabakova. Early post-impact time dynamics of viscous drops onto a solid dry surface. *Physics of Fluids*, 21(3):032101, 2009.

[34] CHR Mundo, M Sommerfeld, and C Tropea. Droplet-wall collisions: experimental studies of the deformation and breakup process. *International journal of multiphase flow*, 21(2):151–173, 1995.

[35] M Pasandideh-Fard, YM Qiao, Sanjeev Chandra, and Javad Mostaghimi. Capillary effects during droplet impact on a solid surface. *Physics of fluids*, 8(3):650–659, 1996.

[36] Rachel E Pepper, Laurent Courbin, and Howard A Stone. Splashing on elastic membranes: The importance of early-time dynamics. *Physics of Fluids*, 20(8):082103, 2008.

[37] DH Peregrine. The fascination of fluid mechanics. *Journal of Fluid Mechanics*, 106:59–80, 1981.

[38] Martin Rein. Phenomena of liquid drop impact on solid and liquid surfaces. *Fluid Dynamics Research*, 12(2):61, 1993.

[39] R Rioboo, M Marengo, and C Tropea. Time evolution of liquid drop impact onto solid, dry surfaces. *Experiments in fluids*, 33(1):112–124, 2002.

[40] Romain Rioboo, Cameron Tropea, and Marco Marengo. Outcomes from a drop impact on solid surfaces. *Atomization and sprays*, 11(2), 2001.

[41] Romain Rioboo, Michel Voue, Helena Adao, Joséphine Conti, Alexandre Vaillant, David Seveno, and Joel De Coninck. Drop impact on soft surfaces: Beyond the static contact angles. *Langmuir*, 26(7):4873–4879, 2010.

[42] Ilia V Roisman. Inertia dominated drop collisions. ii. an analytical solution of the navier–stokes equations for a spreading viscous film. *Physics of Fluids*, 21(5):052104, 2009.

[43] S Rosenblat and SH Davis. How do liquid drops spread on solids? In *Frontiers in fluid mechanics*, pages 171–183. Springer, 1985.

[44] John R Saylor and Garrett D Bounds. Experimental study of the role of the weber and capillary numbers on mesler entrainment. *AIChE journal*, 58(12):3841–3851, 2012.

[45] YA Semenov, GX Wu, and AA Korobkin. Impact of liquids with different densities. *Journal of Fluid Mechanics*, 766:5–27, 2015.

[46] Constantinos Spandagos, Thomas B Goudoulas, Paul F Luckham, and Omar K Matar. Surface tension-induced gel fracture. part 2. fracture of gelatin gels. *Langmuir*, 28(21):8017–8025, 2012.

[47] C Stanley, R Jackson, N Karwa, and G Rosengarten. The effects of surface wettability on droplet fingering. In *The Proceedings of the 19th Australasian Fluid Mechanics Conference*, 2014.

[48] C David Stow and Mark G Hadfield. An experimental investigation of fluid flow resulting from the impact of a water drop with an unyielding dry surface. *Proceedings of the Royal Society of London. A. Mathematical and Physical Sciences*, 373(1755):419–441, 1981.

[49] ST Thoroddsen. The ejecta sheet generated by the impact of a drop. *Journal of Fluid Mechanics*, 451:373–381, 2002.

[50] Annalisa Tirella, Federico Vozzi, Carmelo De Maria, Giovanni Vozzi, Tazio Sandri, Duccio Sassano, Livio Cognolato, and Arti Ahluwalia. Substrate stiffness influences high resolution printing of living cells with an ink-jet system. *Journal of bioscience and bioengineering*, 112(1):79–85, 2011.

[51] Visakh Vaikuntanathan and D Sivakumar. Maximum spreading of liquid drops impacting on groove-textured surfaces: effect of surface texture. *Langmuir*, 32(10):2399–2409, 2016.

[52] Dirkjan B van Dam and Christophe Le Clerc. Experimental study of the impact of an ink-jet printed droplet on a solid substrate. *Physics of Fluids*, 16(9):3403–3414, 2004.

[53] EJ Vega and AA Castrejón-Pita. Suppressing prompt splash with polymer additives. *Experiments in Fluids*, 58(5):57, 2017.

[54] An-Bang Wang and Chi-Chang Chen. Splashing impact of a single drop onto very thin liquid films. *Physics of fluids*, 12(9):2155–2158, 2000.

[55] Daniel A Weiss and Alexander L Yarin. Single drop impact onto liquid films: neck distortion, jetting, tiny bubble entrainment, and crown formation. *Journal of Fluid Mechanics*, 385:229–254, 1999.

[56] John S Wettlaufer and Eric R Dufresne. Stiffening solids with liquid inclusions. *Soft Matter*, 11:672, 2015.

[57] Arthur Mason Worthington and Reginald Sorrè Cole. V. impact with a liquid surface, studied by the aid of instantaneous photography. *Philosophical Transactions of the Royal Society of London. Series A, Containing Papers of a Mathematical or Physical Character*, (189):137–148, 1897.

[58] Lei Xu. Liquid drop splashing on smooth, rough, and textured surfaces. *Physical Review E*, 75(5):056316, 2007.

[59] Lei Xu, Loreto Barcos, and Sidney R Nagel. Splashing of liquids: Interplay of surface roughness with surrounding gas. *Physical Review E*, 76(6):066311, 2007.

[60] Lei Xu and Sidney R Nagel. Controlling the direction and amount of a splash with textured surface. *arXiv preprint physics/0702098*, 2007.